Nanoscale

COMMUNICATION

View Article Online
View Journal | View Issue

Cite this: *Nanoscale*, 2019, **11**, 21733

Received 26th June 2019,
Accepted 4th November 2019

DOI: 10.1039/c9nr09347h

rsc.li/nanoscale

On the role of helper lipids in lipid nanoparticle formulations of siRNA†

Jayesh A. Kulkarni, *[a,b] Dominik Witzigmann, [a] Jerry Leung,[a] Yuen Yi C. Tam[a] and Pieter R. Cullis *[a,c]

Onpattro, the first RNAi-based therapeutic to receive FDA approval, is enabled by a lipid nanoparticle (LNP) system that facilitates siRNA delivery into the cytoplasm of target cells (hepatocytes) following intravenous (i.v.) administration. These LNP-siRNA systems consist of four lipid components (ionizable cationic lipid, distearolyphosphatidycholine or DSPC, cholesterol, and PEG-lipid) and siRNA. The ionizable cationic lipid has been optimised for RNA encapsulation and intracellular delivery, and the PEG-lipids have been engineered to regulate LNP size and transfection potency. The roles of the other "helper" lipids, DSPC and cholesterol, remain less clear. Here we show that in empty LNP systems that do not contain siRNA, DSPC–cholesterol resides in outer layers, whereas in loaded systems a portion of the DSPC–cholesterol is internalised together with siRNA. It is concluded that the presence of internalised helper lipid is vital to the stable encapsulation of siRNA in the LNP and thus to LNP-siRNA function.

The lipid nanoparticle (LNP) system employed by Onpattro, the first RNAi drug approved by the FDA, contains ionizable cationic lipid, distearolyphosphatidycholine (DSPC), cholesterol and PEG-lipid and facilitates delivery of encapsulated siRNA into hepatocytes following systemic administration.[1–3] The ionizable cationic lipid has been optimized for maximum gene silencing employing an *in vivo* FVII model,[4,5] and the PEG-lipids have been designed to regulate LNP size without compromising transfection properties.[6,7] In this study we investigate the roles of the "helper" lipids, DSPC and cholesterol. We show that the presence of helper lipid is vital to the stable encapsulation of siRNA in the LNP by participating in the formation of internalized siRNA-lipid complexes.

Initial studies focused on the distribution of DSPC–cholesterol in empty LNP systems. Previous studies[8,9] indicate that DSPC is primarily located in the outer monolayer surrounding the hydrophobic core of the LNP and that cholesterol has limited solubility in the ionizable lipid oil at pH 7.4;[9] therefore, it must reside primarily either in combination with DSPC or in the form of cholesterol crystals. Such crystals have been observed experimentally for the "clinical" LNP composition consisting of MC3/Chol/DSPC/PEG-lipid (50/39/10/1 mol%),[8] suggesting that the amount of cholesterol exceeds the amount that can be stably dissolved in the LNP. Numerous studies have shown that cholesterol forms a stable "liquid-ordered" structure[10] with DSPC at levels up to ~1 : 1 (mol : mol).[11–13] In order to avoid ambiguities resulting from the presence of excess cholesterol, it was decided to maintain the DSPC–cholesterol ratio at 1 : 1 (mol : mol) and to investigate the morphology of the LNP as the proportion of DSPC/cholesterol was increased in relation to the amount of ionizable cationic lipid.

LNP systems were generated containing 5 to 80 mol% DSPC–cholesterol (1 : 1 mol) where the amount of ionizable cationic lipid was reduced from 94 mol% to 19 mol% as the DSPC–cholesterol content was raised. The PEG-lipid was maintained at 1 mol%. The ionizable cationic lipid employed was 2,2-dilinoleyl-4-(2-dimethylaminoethyl)-[1,3]-dioxolane (KC2).[5] As noted in Fig. 1, the LNP showed typical "solid-core" structures that decreased in size as the DSPC–cholesterol content was increased from 5 mol% to 60 mol% and then exhibited a remarkable hybrid solid core within a lipid bilayer morphology for LNP containing 80 mol% DSPC–cholesterol (Fig. 1E). Assuming that the inner solid core of the hybrid structure (average diameter ~30 nm) consists solely of KC2 surrounded first by a monolayer of DSPC–cholesterol and then by an outer bilayer consisting entirely of DSPC–cholesterol, the theoretical

[a]*Department of Biochemistry and Molecular Biology, University of British Columbia, 2350 Health Sciences Mall, Vancouver, British Columbia, Canada, V6T 1Z3. E-mail: j.kulkarni@alumni.ubc.ca, pieterc@mail.ubc.ca; Fax: +1 (604)-822-4843; Tel: +1 (604)-822-4144*

[b]*Department of Medical Genetics, University of British Columbia, Center for Molecular Medicine and Therapeutics, 950 West 28th Avenue, Vancouver, British Columbia, V5Z 4H4, Canada*

[c]*NanoMedicines Innovation Network (NMIN), 2350 Health Sciences Mall, University of British Columbia, Vancouver, BC V6T 1Z3 Canada*

†Electronic supplementary information (ESI) available. See DOI: 10.1039/c9nr09347h

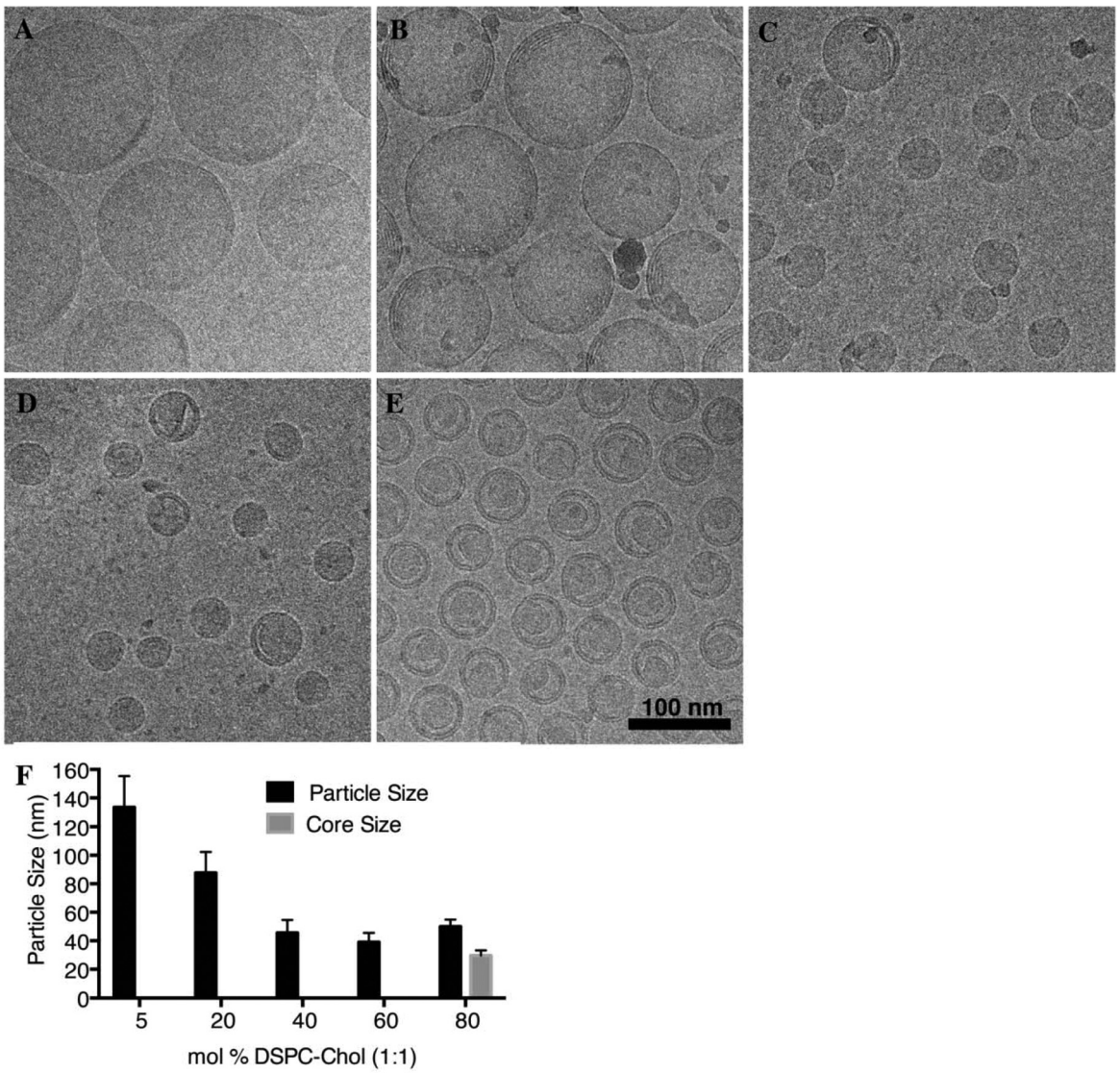

Fig. 1 The DSPC–cholesterol content dramatically modulates LNP morphology. LNP formulations composed of KC2/DSPC/Chol/PEG-lipid were prepared in pH4 buffer and dialyzed into PBS, pH 7.4. The resulting particles were imaged by cryo-TEM (A–E). All formulations contained DSPC–chol at a 1 : 1 mol ratio and 1 mol% PEG-lipid. The combined DSPC–chol (1 : 1 mol) content was 5% (A), 20% (B), 40% (C), 60% (D) and 80% (E). Scale bar = 100 nm. (F) Particle sizes were obtained by manual sizing from cryo-TEM micrographs of LNP formulations (n = 200). Results represent mean ± standard deviation. For the formulation containing 19 mol% KC2, the size of the dense inner core was also measured.

size of the high DSPC–cholesterol hybrid systems can be calculated to be 50 nm, assuming a combined DSPC–cholesterol area per molecule[3] of 0.85 nm^2 and that the inner core inside the monolayer of DSPC–cholesterol consists solely of KC2 oil at a density of 0.9 g mL^{-1}. This is close to the observed size of 49 nm (Fig. 1F). These results support the proposal that at low levels DSPC–cholesterol forms a monolayer around the neutral ionizable lipid oil core of the empty LNP system and, when the amount of DSPC–cholesterol present exceeds the amount required to coat the hydrophobic core, forms bilayer blebs that eventually form complete bilayers around the central core lipid and an entrapped aqueous volume.

The results shown in Fig. 1 also demonstrate that as the proportion of DSPC–cholesterol is increased, the "solid core" LNP produced become considerably smaller until a limiting size of ~40 nm is reached, at which point the bilayer blebs begin to appear. This finding indicates that the DSPC–cholesterol content also modulates LNP size, as would be expected if it resides primarily in the surface monolayer. Previous work has assumed that the primary determinant of LNP-siRNA size is the PEG-lipid content which can dramatically modulate LNP size as the amount of PEG-lipid is varied from 1–5 mol%.[14,15] It is of interest to determine whether there is sufficient DSPC in clinical LNP-siRNA formulations to form a monolayer into which the PEG-lipid is embedded, around the core structure. The lipid mixture used clinically contains 1.5 mol% PEG-lipid and 10 mol% DSPC and exhibits a net size of ~45 nm diameter by cryo-TEM.[15] Assuming that the DSPC is all located in the

outer monolayer and is associated with maximum possible levels of cholesterol (2 : 1 cholesterol : DSPC; mol/mol)[10] with limiting area per molecule of 0.6 nm^2 for DSPC and 0.25 nm^2 for cholesterol[16] and that the remaining cholesterol and KC2 is present in the hydrophobic core at a density of 0.9 g mL^{-1}, the diameter of an LNP composed of KC2/DSPC/Chol/PEG-lipid (50/10/39/1 mol%) can be calculated to be ~50 nm, suggesting that the DSPC content is close to the equilibrium value required to form a surface monolayer around the empty LNP.

In order to further demonstrate that LNP structure reflects the relative surface lipid content (PEG-lipid and DSPC–cholesterol), LNP morphology was monitored for the ionizable lipid/DSPC/Chol/PEG-lipid composition used clinically (50/10/38.5/1.5; mol%) where the PEG-lipid content was varied over the range 0.5–2.5 mol%. As expected, the LNP become smaller as the PEG-lipid content is increased (Fig. 2). However, the LNP containing low (0.5 mol%) levels of PEG-lipid display pronounced bilayer protrusions. These LNP are larger (58 nm diameter) than the equilibrium value of ~50 nm if all the DSPC is present in the outer monolayer. Thus, the results suggest that the amount of DSPC–cholesterol for the LNP containing 0.5 mol% PEG-lipid is in excess of the amount required to form a surface monolayer, leading to the bilayer blebs. As the amount of PEG-lipid is increased and the size decreases this imbalance is reduced, leading to the reduced occurrence of blebs at higher PEG contents, as observed.

The next question concerns the influence of the siRNA payload on the intraparticle distribution of helper lipids. In order to investigate this, we chose to study LNP siRNA systems with high contents of siRNA where the effects of siRNA on LNP structure and the distribution of lipids within that structure would be most apparent. As noted previously,[9] at high siRNA contents (lipid amine-to-oligonucleotide phosphate (N/P) ratios of one), LNP siRNA systems with the "clinical" lipid composition appear as a series of concentric bilayers as visualized by cryo-TEM, consistent with sequestration of siRNA between closely apposed lipid bilayers.[17–19] While optimized LNP siRNA activity requires excess ionizable cationic lipid (N/P values >3),[14,20] the LNP siRNA complexes observed at both N/P = 1 and N/P = 3 exhibit the same bilayer signature as detected by small angle X-ray techniques,[9] indicating they reflect the same structure.

We examined the morphology and encapsulation efficiencies of LNP loaded with siRNA at N/P = 1 for the range of lipid compositions used for the empty preparations of Fig. 1. As shown in Fig. 3, the LNP-siRNA systems produced exhibit dramatically different morphologies compared to the "empty" systems. At low DSPC–cholesterol levels (5 mol% DSPC–cholesterol and 20 mol% DSPC–cholesterol) low encapsulation efficiencies and large systems with some internal concentric or stacked bilayer structures are observed. For systems containing 40 and 60 mol% DSPC–cholesterol high encapsulation efficiencies are achieved and tightly packed concentric multilamellar systems are observed. Finally, at very high DSPC–cholesterol levels (80 mol%) larger systems with less tightly packed lamellae are observed, however high trapping efficiencies are maintained. The corresponding particle sizes are presented in ESI Fig. 1.†

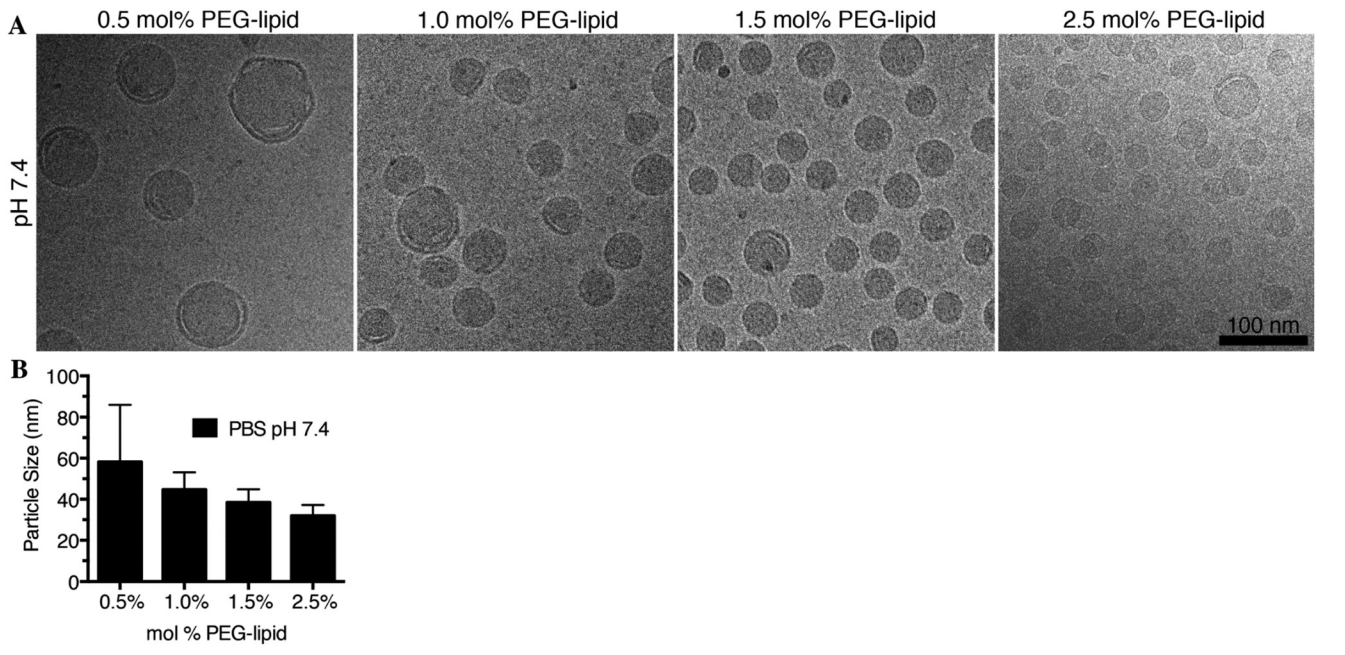

Fig. 2 Influence of PEG-lipid content on LNP morphology and size (A) Cryo-TEM micrographs of LNP composed of KC2/DSPC/Chol/PEG-lipid at molar ratios of 50/10/37.5–39.5/0.5–2.5 (respectively). These LNP were prepared in pH 4 buffer through rapid-mixing and dialyzed into PBS pH 7.4 to remove solvent and neutralize the pH. Scale bar = 100 nm. (B) Particle sizes of LNP at pH 7.4 as determined by manual measurement of 200 particles as visualized by cryo-TEM. Results indicate mean ± standard deviation.

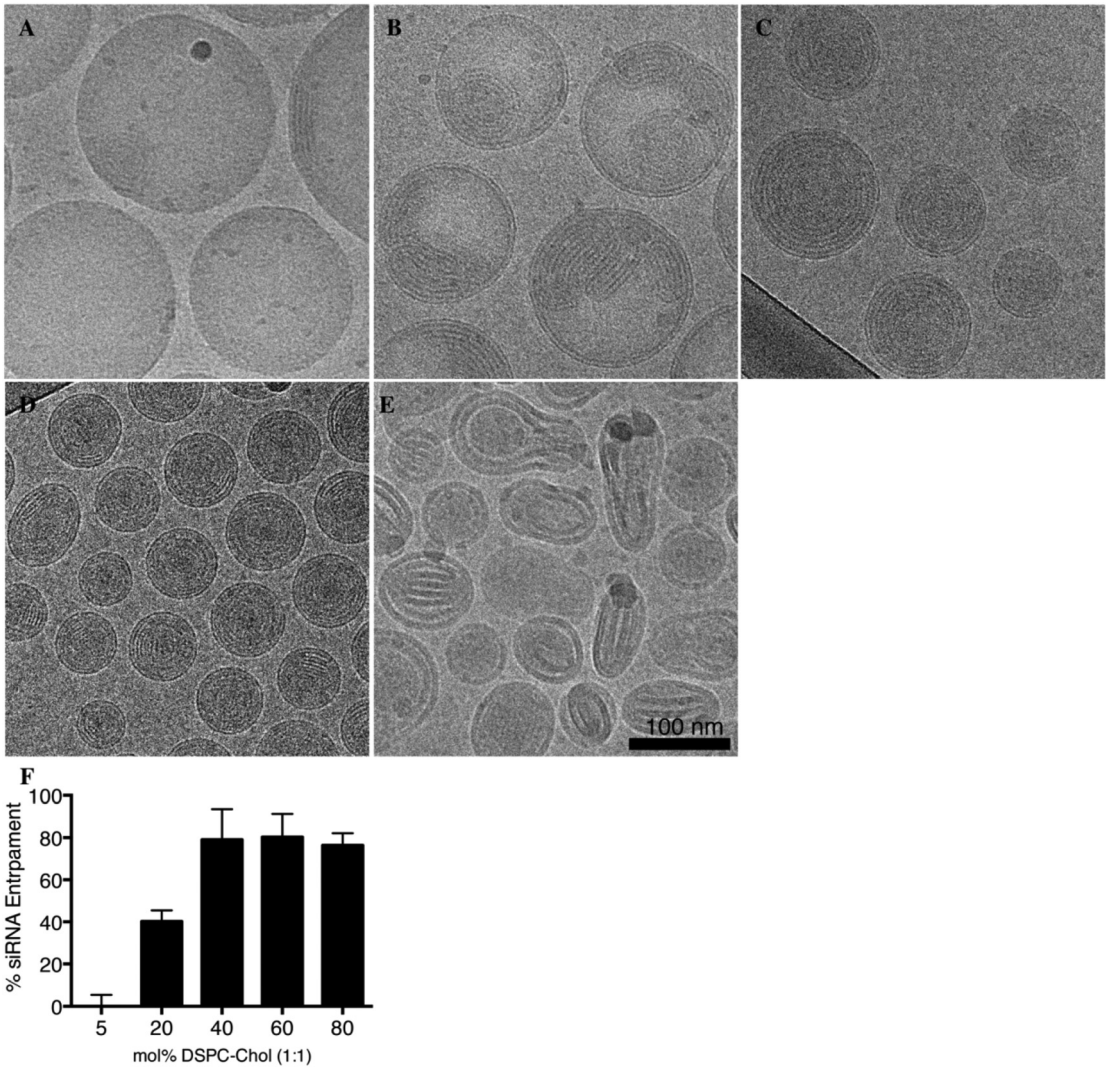

Fig. 3 High siRNA contents induce dramatic changes in LNP morphology consistent with the formation of lipid-siRNA structures that contain helper lipid. LNP siRNA formulations were generated through rapid mixing of an aqueous medium (sodium acetate pH 4) containing luciferase siRNA with an ethanol medium containing KC2, DSPC, Chol and PEG-lipid. The ionizable amino lipid to oligonucleotide phosphate N/P ratio was 1. The formulations contained DSPC–chol at a 1 : 1 mol ratio and 1 mol% PEG-lipid where the DSPC–chol content was increased at the expense of the KC2 content. The lipid composition (KC2/DSPC/Chol/PEG-lipid; mol%) of the LNP visualized in the cryo-TEM micrographs was (A) 94/2.5/2.5/1, (B) 79/10/10/1, (C) 59/20/20/1, (D) 39/30/30/1 and (E) 19/40/40/1. Scale bar = 100 nm. (F) DSPC–cholesterol is required for effective siRNA encapsulation. siRNA entrapment was measured as a function of the amounts of DSPC–cholesterol present using an RNA-binding dye-exclusion assay detailed in the Methods section. Results indicate mean ± standard deviation (n = 3).

The data presented in Fig. 3 support three conclusions. First, the presence of siRNA clearly converts associated ionizable lipid into a form that prefers bilayer structure even at neutral pH values. This is indicated by the absence of the amorphous solid core as well as the clear lamellar structures observed in all cryo-TEM images. Second, the loaded LNP systems are considerably larger than the unloaded systems, suggesting that a proportion of the DSPC–cholesterol is located inside the LNP and is not available as surface lipid. Third, at low DSPC–cholesterol contents (lower than ~40 mol%) the siRNA encapsulation efficiency is progressively reduced (Fig. 3F), indicating that the relative lack of DSPC–cholesterol limits the amount of siRNA that can be encapsulated, again indicating an association between internalized siRNA and DSPC–cholesterol. The overall conclusion is therefore that a proportion of the DSPC–cholesterol is contained in the lipid complex with siRNA.

The simplest hypothesis for the mechanism of formation of the concentric bilayer structures noted for DSPC–cholesterol contents of 40 and 60 mol% (Fig. 3C and D) consists first of production of an initial positively charged nucleating bilayer vesicle at pH 4 (note these lipid compositions form small vesicular structures at pH 4)[9] followed by deposition of siRNA on the vesicle surface by charge association to result in a net

negative surface charge, followed by deposition of a subsequent positively charged bilayer vesicle and so on until essentially all the siRNA has been segregated into the LNP structure. The surface charge density on the siRNA can be calculated as approximately −0.9 q nm^{-2} for a 21-mer duplex (diameter 2 nm, length 7.5 nm).[21] The surface charge density on the lipid membrane obviously depends on the proportion of positively charged KC2 present. Interestingly, the encapsulation efficiency starts to decrease at DSPC–cholesterol contents below 40 mol% corresponding to KC2 concentrations above 60 mol%, suggesting a maximum membrane surface charge density for efficient encapsulation that is just above ~+0.8 q nm^{-2}. This calculation assumes an area per molecule of 0.85 nm^2 for the DSPC–cholesterol complex and 0.7 nm^2 for the positively charged KC2. The area per molecule of KC2 has not been determined, however the area per molecule of dilinoleoyl phosphatidylcholine is 0.7 nm^2.[22] A logical interpretation of the data is therefore that productive encapsulation of siRNA at pH 4 that is maintained at pH 7.4 requires formation of a structure where the negatively charged siRNA is sandwiched between two positively charged bilayers where the surface charge density on the lipid bilayers is equal and opposite to the surface charge density exhibited by the siRNA. Using the assumptions noted above, it can be calculated that in order for the lipid bilayer to exhibit a surface charge equal and opposite to the surface charge on the siRNA (−0.9 q nm^{-2}) the lipid composition associated with the siRNA would consist of 33 mol% DSPC–cholesterol and 66 mol% KC2. If the positive surface charge on the membrane is higher than +0.9 q nm^{-2} it may be hypothesized that the "zippering" effect between two bilayers triggered by siRNA that results in stable encapsulation is less effective due to residual inter-bilayer electrostatic repulsion effects.

It is likely that a variety of polar "helper" lipids can satisfy the need for diluting the cationic lipid content to the point where productive encapsulation can occur. In order to test this the encapsulation properties of LNP-siRNA systems containing the polar lipids dioleoyl phosphatidylethanolamine (DOPE), dioleoylphosphatidylcholine (DOPC), egg sphingomyelin (ESM) and cholesterol were compared to LNP containing non-polar triglyceride lipids (triolein, and trilinolein). As shown in ESI Fig. 2,† incorporation of DOPE, DOPC, ESM and cholesterol allow effective entrapment of siRNA, but triolein and trilinolein are ineffective. It is often suggested that helper lipids such as DOPE enhance intracellular delivery by promoting non-bilayer structures, however the results presented here would argue that their role in achieving stable oligonucleotide encapsulation could be of primary importance.

It is of interest to consider the implications of these results for the structure and function of LNP-siRNA delivery systems used clinically, for which the siRNA/lipid weight ratio is 0.098 (ref. 23) corresponding to an N/P ratio of three. This implies that ~30% of the ionizable lipid is complexed with siRNA and is present in an internalized bilayer form. Assuming that this complex consists of DSPC–cholesterol and ionizable lipid at a 1 : 2 ratio to achieve charge neutralization, it may be calculated that nearly 50% of the DSPC in the LNP-siRNA system is present in internalized complexes rather than residing on the LNP surface. It is probable that this distribution contributes to the surface properties of the LNP as well as particle instability.

In summary, the results of this study indicate that helper lipids such as DSPC–cholesterol play essential roles in LNP-siRNA systems by participating in the formation of siRNA-lipid complexes that remain stable at neutral pH, thus enabling encapsulation of siRNA. Such complexes appear essential to the function of clinically approved LNP-siRNA systems.

Materials and methods

Materials

The lipids 1,2-distearoyl-*sn-glycero*-3-phosphocholine (DSPC), 1,2-dioleoyl-*sn-glycero*-3-phosphoethanolamine (DOPE), egg sphingomyelin (ESM), 1,2-dioleoyl-*sn-glycero*-3-phosphocholine (DOPC), and 1,2-distearoyl-*sn-glycero*-3-phosphoethanolamine-*N*-[methoxy(polyethylene glycol)-2000] (ammonium salt) (PEG-DSPE) were purchased from Avanti Polar Lipids (Alabaster, AL). The ionizable amino-lipid 2,2-dilinoleyl-4-(2-dimethylaminoethyl)-[1,3]-dioxolane (KC2) was synthesized by Biofine International (Vancouver, BC). Cholesterol, triolein, and trilinolein were purchased from Sigma-Aldrich (St Louis, MO). (*R*)-2,3-Bis(tetradecyloxy)propyl-1-(methoxy polyethylene glycol 2000) carbamate (PEG-DMG) was synthesized as previously described.[24] TEM grids were purchased from Ted Pella, Inc. (Redding, CA). siRNA against firefly luciferase[25] (as a control, non-target siRNA) was purchased from IDT (Coralville, IA) with the sequence S: cuuAcGcuGAGuAcuucGAdTsdT, AS: UCGAAGuACUcAGCGuAAGdTsdT. The modifications are phosphorothioate linkages (indicated as the letter "s") between the 3′-deoxythymidine (dT) overhangs and includes multiple 2′-OMe modifications (indicated by lower-case letters). In previous work,[15,17,20] replacing this siRNA with alternative sequences had no effect on particle morphology.

Preparation of empty LNP

LNP were prepared as previously described.[9,26,27] Briefly, lipid components (KC2, Chol, DSPC, and PEG-lipid) at appropriate ratios were dissolved in ethanol to a concentration of 10–15 mM total lipid. The aqueous phase consisted of 25 mM sodium acetate pH 4 buffer. The two solutions were mixed through a T-junction mixer[28,29] at a total flow rate of 20 mL min^{-1}, and a flow rate ratio of 3 : 1 v/v (corresponding to 15 : 5 mL min^{-1} aqueous : organic phase). Unless otherwise specified, the resulting suspension was subsequently dialysed against 1000-fold volume of the same sodium acetate pH 4 buffer or against phosphate buffered saline (PBS pH 7.4).

Preparation of LNP containing nucleic acid

LNP-nucleic acid were prepared as previously described.[9,26,27] Briefly, lipid components (KC2, Chol, DSPC, and PEG-lipid) at appropriate ratios were dissolved in ethanol to a concentration of 10 mM total lipid. Purified nucleic acid polymers were dis-

solved in 25 mM sodium acetate pH 4 buffer to achieve the desired N/P ratio. The two solutions were mixed through a T-junction mixer[28,29] at a total flow rate of 20 mL min^{-1}, and a flow rate ratio of 3 : 1 v/v (aqueous : organic phase). The resulting suspension was subsequently dialyzed against the acetate pH 4 buffer or directly against PBS pH 7.4.

Cryogenic transmission electron microscopy (cryo-TEM)

Cryo-TEM was performed as previously described.[9] LNP suspensions were concentrated to a final concentration of 20–25 mg mL^{-1} of total lipid and added to glow-discharged copper grids (3–5 μL), and plunge-frozen using a FEI Mark IV Vitrobot (FEI, Hillsboro, OR) to generate vitreous ice. Grids were stored in liquid nitrogen until imaged. An FEI LaB6 G2 TEM (FEI, Hillsboro, OR) was used to image all samples. The instrument was operating at 200 kV under low-dose conditions. A bottom-mount FEI Eagle 4K CCD camera was used to capture all images. All samples (unless otherwise stated) were imaged at a 55 000× magnification with a nominal underfocus of 1–2 μm to enhance contrast. Sample preparation and imaging was performed at the UBC Bioimaging Facility (Vancouver, BC).

Analysis of LNPs

Cryo-TEM micrographs obtained for each sample were characterized for particle size (as compared by length to the scale bar), performed by manual counting of at least 150 LNPs to account for scattering interference from different morphology. In some cases, dynamic light scattering was performed on a Malvern Zetasizer Nano ZS. This technique has been shown to closely correlate with the number-weighted average produced by dynamic light scattering.[15] Similarly, the proportion of LNPs in the dumbbell or bilamellar morphology was determined manually. Lipid concentrations were measured using the Cholesterol E Total-Cholesterol assay (Wako Diagnostics, Richmond, VA). RNA entrapment was measured using the procedure described elsewhere.[17]

Conflicts of interest

The authors have no conflicts to declare.

Acknowledgements

PRC acknowledges support from the Canadian Institutes for Health Research (FDN 148469). DW acknowledges the support of the Swiss National Science Foundation (SNF, Early Postdoc. Mobility Fellowship, Grant No. 174975). JL is supported by a Frederick Banting and Charles Best Canada Graduate Scholarship – Masters (6556). PRC is the Scientific Director and CEO of the NanoMedicines Innovation Network, a Canadian Network of Centres of Excellence.

References

1 Alnylam® Pharmaceuticals, I., Alnylam Announces First-Ever Fda Approval of an Rnai Therapeutic, Onpattro™ (Patisiran) for the Treatment of the Polyneuropathy of Hereditary Transthyretin-Mediated Amyloidosis in Adults. http://investors.alnylam.com/news-releases/news-release-details/alnylam-announces-first-ever-fda-approval-rnai-therapeutic, 2018.

2 Alnylam® Pharmaceuticals., I., Alnylam Initiates Phase I Clinical Study of Aln-Ttr02, an Rnai Therapeutic Targeting Transthyretin (Ttr) for the Treatment of Ttr-Mediated Amyloidosis (Attr). http://investors.alnylam.com/news-releases/news-release-details/alnylam-initiates-phase-i-clinical-study-aln-ttr02-rnai, 2012.

3 T. Miyoshi and S. Kato, Detailed Analysis of the Surface Area and Elasticity in the Saturated 1,2-Diacylphosphatidylcholine/Cholesterol Binary Monolayer System, *Langmuir*, 2015, **31**, 9086–9096.

4 M. Jayaraman, S. M. Ansell, B. L. Mui, Y. K. Tam, J. Chen, X. Du, D. Butler, L. Eltepu, S. Matsuda, J. K. Narayanannair, K. G. Rajeev, I. M. Hafez, A. Akinc, M. A. Maier, M. A. Tracy, P. R. Cullis, T. D. Madden, M. Manoharan and M. J. Hope, Maximizing the Potency of Sirna Lipid Nanoparticles for Hepatic Gene Silencing in Vivo, *Angew. Chem., Int. Ed.*, 2012, **51**, 8529–8533.

5 S. C. Semple, A. Akinc, J. Chen, A. P. Sandhu, B. L. Mui, C. K. Cho, D. W. Sah, D. Stebbing, E. J. Crosley, E. Yaworski, I. M. Hafez, J. R. Dorkin, J. Qin, K. Lam, K. G. Rajeev, K. F. Wong, L. B. Jeffs, L. Nechev, M. L. Eisenhardt, M. Jayaraman, *et al.*, Rational Design of Cationic Lipids for Sirna Delivery, *Nat. Biotechnol.*, 2010, **28**, 172–176.

6 E. Ambegia, S. Ansell, P. Cullis, J. Heyes, L. Palmer and I. MacLachlan, Stabilized Plasmid-Lipid Particles Containing Peg-Diacylglycerols Exhibit Extended Circulation Lifetimes and Tumor Selective Gene Expression, *Biochim. Biophys. Acta*, 2005, **1669**, 155–163.

7 J. Heyes, K. Hall, V. Tailor, R. Lenz and I. MacLachlan, Synthesis and Characterization of Novel Poly(Ethylene Glycol)-Lipid Conjugates Suitable for Use in Drug Delivery, *J. Controlled Release*, 2006, **112**, 280–290.

8 M. Yanez Arteta, T. Kjellman, S. Bartesaghi, S. Wallin, X. Wu, A. J. Kvist, A. Dabkowska, N. Szekely, A. Radulescu, J. Bergenholtz and L. Lindfors, Successful Reprogramming of Cellular Protein Production through Mrna Delivered by Functionalized Lipid Nanoparticles, *Proc. Natl. Acad. Sci. U. S. A.*, 2018, **115**, E3351–E3360.

9 J. A. Kulkarni, M. M. Darjuan, J. E. Mercer, S. Chen, R. van der Meel, J. L. Thewalt, Y. Y. C. Tam and P. R. Cullis, On the Formation and Morphology of Lipid Nanoparticles Containing Ionizable Cationic Lipids and Sirna, *ACS Nano*, 2018, **12**, 4787–4795.

10 J. Huang, J. T. Buboltz and G. W. Feigenson, Maximum Solubility of Cholesterol in Phosphatidylcholine and Phosphatidylethanolamine Bilayers, *Biochim. Biophys. Acta*, 1999, **1417**, 89–100.

11 A. Parker, K. Miles, K. H. Cheng and J. Huang, Lateral Distribution of Cholesterol in Dioleoylphosphatidylcholine Lipid Bilayers: Cholesterol-Phospholipid Interactions at High Cholesterol Limit, *Biophys. J.*, 2004, **86**, 1532–1544.
12 A. Magarkar, V. Dhawan, P. Kallinteri, T. Viitala, M. Elmowafy, T. Róg and A. Bunker, Cholesterol Level Affects Surface Charge of Lipid Membranes in Saline Solution, *Sci. Rep.*, 2014, **4**, 5005.
13 D. Bach and E. Wachtel, Phospholipid/Cholesterol Model Membranes: Formation of Cholesterol Crystallites, *Biochim. Biophys. Acta*, 2003, **1610**, 187–197.
14 N. M. Belliveau, J. Huft, P. J. Lin, S. Chen, A. K. Leung, T. J. Leaver, A. W. Wild, J. B. Lee, R. J. Taylor, Y. K. Tam, C. L. Hansen and P. R. Cullis, Microfluidic Synthesis of Highly Potent Limit-Size Lipid Nanoparticles for in Vivo Delivery of Sirna, *Mol. Ther. – Nucleic Acids*, 2012, **1**, e37.
15 S. Chen, Y. Y. Tam, P. J. Lin, A. K. Leung, Y. K. Tam and P. R. Cullis, Development of Lipid Nanoparticle Formulations of Sirna for Hepatocyte Gene Silencing Following Subcutaneous Administration, *J. Controlled Release*, 2014, **196**, 106–112.
16 C. L. Armstrong, D. Marquardt, H. Dies, N. Kucerka, Z. Yamani, T. A. Harroun, J. Katsaras, A. C. Shi and M. C. Rheinstadter, The Observation of Highly Ordered Domains in Membranes with Cholesterol, *PLoS One*, 2013, **8**, e66162.
17 S. Chen, Y. Y. Tam, P. J. Lin, M. M. Sung, Y. K. Tam and P. R. Cullis, Influence of Particle Size on the in Vivo Potency of Lipid Nanoparticle Formulations of Sirna, *J. Controlled Release*, 2016, **235**, 236–244.
18 S. Chen, J. Zaifman, J. A. Kulkarni, I. V. Zhigaltsev, Y. K. Tam, M. A. Ciufolini, Y. Y. C. Tam and P. R. Cullis, Dexamethasone Prodrugs as Potent Suppressors of the Immunostimulatory Effects of Lipid Nanoparticle Formulations of Nucleic Acids, *J. Controlled Release*, 2018, **286**, 46–54.
19 B. L. Mui, Y. K. Tam, M. Jayaraman, S. M. Ansell, X. Du, Y. Y. Tam, P. J. Lin, S. Chen, J. K. Narayanannair, K. G. Rajeev, M. Manoharan, A. Akinc, M. A. Maier, P. Cullis, T. D. Madden and M. J. Hope, Influence of Polyethylene Glycol Lipid Desorption Rates on Pharmacokinetics and Pharmacodynamics of Sirna Lipid Nanoparticles, *Mol. Ther. – Nucleic Acids*, 2013, **2**, e139.
20 A. K. Leung, I. M. Hafez, S. Baoukina, N. M. Belliveau, I. V. Zhigaltsev, E. Afshinmanesh, D. P. Tieleman, C. L. Hansen, M. J. Hope and P. R. Cullis, Lipid Nanoparticles Containing Sirna Synthesized by Microfluidic Mixing Exhibit an Electron-Dense Nanostructured Core, *J. Phys. Chem. C*, 2012, **116**, 18440–18450.
21 J. M. Rosenberg, N. C. Seeman, R. O. Day and A. Rich, Rna Double Helices Generated from Crystal Structures of Double Helical Dinucleoside Phosphates, *Biochem. Biophys. Res. Commun.*, 1976, **69**, 979–987.
22 J. M. Smaby, M. M. Momsen, H. L. Brockman and R. E. Brown, Phosphatidylcholine Acyl Unsaturation Modulates the Decrease in Interfacial Elasticity Induced by Cholesterol, *Biophys. J.*, 1997, **73**, 1492–1505.
23 Alnylam® Pharmaceuticals, I., Onpattro Prescribing Information. https://www.alnylam.com/wp-content/uploads/2018/08/ONPATTRO-Prescribing-Information.pdf, 2018.
24 A. Akinc, A. Zumbuehl, M. Goldberg, E. S. Leshchiner, V. Busini, N. Hossain, S. A. Bacallado, D. N. Nguyen, J. Fuller, R. Alvarez, A. Borodovsky, T. Borland, R. Constien, A. de Fougerolles, J. R. Dorkin, K. Narayanannair Jayaprakash, M. Jayaraman, M. John, V. Koteliansky, M. Manoharan, *et al.*, A Combinatorial Library of Lipid-Like Materials for Delivery of Rnai Therapeutics, *Nat. Biotechnol.*, 2008, **26**, 561–569.
25 G. Basha, M. Ordobadi, W. R. Scott, A. Cottle, Y. Liu, H. Wang and P. R. Cullis, Lipid Nanoparticle Delivery of Sirna to Osteocytes Leads to Effective Silencing of Sost and Inhibition of Sclerostin in Vivo, *Mol. Ther. – Nucleic Acids*, 2016, **5**, e363.
26 J. A. Kulkarni, J. L. Myhre, S. Chen, Y. Y. C. Tam, A. Danescu, J. M. Richman and P. R. Cullis, Design of Lipid Nanoparticles for in Vitro and in Vivo Delivery of Plasmid DNA, *Nanomedicine*, 2016, **13**, 1377–1387.
27 J. A. Kulkarni, D. Witzigmann, J. Leung, R. van der Meel, J. Zaifman, M. M. Darjuan, H. M. Grisch-Chan, B. Thöny, Y. Y. C. Tam and P. R. Cullis, Fusion-Dependent Formation of Lipid Nanoparticles Containing Macromolecular Payloads, *Nanoscale*, 2019, **11**, 9023–9031.
28 S. Hirota, C. T. de Ilarduya, L. G. Barron and F. C. Szoka Jr., Simple Mixing Device to Reproducibly Prepare Cationic Lipid-DNA Complexes (Lipoplexes), *BioTechniques*, 1999, **27**, 286–290.
29 J. A. Kulkarni, Y. Y. C. Tam, S. Chen, Y. K. Tam, J. Zaifman, P. R. Cullis and S. Biswas, Rapid Synthesis of Lipid Nanoparticles Containing Hydrophobic Inorganic Nanoparticles, *Nanoscale*, 2017, **9**, 13600–13609.